Journal of the Korean Nuclear Society
Volume 29, Number 4, pp. 310~319, August 1997

Stress Index Development for Piping with Trunnion Attachment Under Pressure and Moment Loadings

Dae-hee Lee, Jong-min Kim, and Sung-ho Park
Korea Power Engineering Company
150 Dukjin-dong, Yusong-gu, Taejon 305-353, Korea

(Received November 19, 1997)

Abstract

A finite element analysis of a trunnion pipe anchor is presented. The structure is analyzed for the case of internal pressure and moment loadings. The stress results are categorized into the average (membrane) stress, the linearly varying (bending) stress and the peak stress through the thickness. The resulting stresses are interpreted per Section III of the ASME Boiler and Pressure Vessel Code from which the Primary(B_1), Secondary(C_1) and Peak(K_1) stress indices for pressure, the Primary (B_2), Secondary(C_2) and Peak(K_2) stress indices for moment are developed. Based on the comparison between stress value by stress indices derived in this paper and stress value represented by the ASME Code Case N-391-1, the empirical equations for stress indices are effectively used in the piping stress analysis. Therefore, the use of empirical equations can simplify the procedure of evaluating the local stress in the piping design stage.

1. Introduction

The support of a piping system for dynamic loads such as seismic load or waterhammer is required to weld an attachment to the pipe to form a part of the supporting structure. These types of configurations are commonly used in nuclear power plants to restraint or anchor the pipe. However, ASME Code Section III [1] does not provide stress indices for these types of configurations. The purpose of this paper is to identify the primary(B_1, B_2), secondary(C_1, C_2) and peak(K_1, K_2) stress indices as defined by the welded trunnions attached to pipe.

The trunnion support is shown in Fig.1. It represents a cylindrical support pipe welded to a run pipe. The trunnion pipe does not penetrate the run pipe in a 90 degree branch connection, and the trunnion pipe is not pressurized. This type of component is similar to an integral attachment.

Stress indices were introduced into the first edition of Section III of the ASME Code (1963) for nozzles in pressure vessels subjected to internal pressure load-

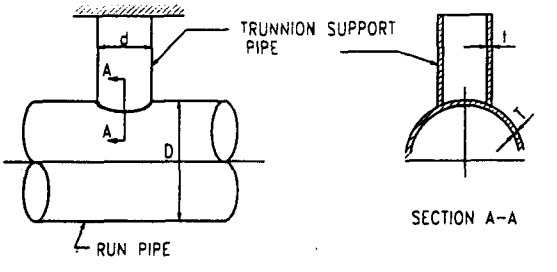

Fig. 1. Typical Trunnion Support

ing only. These indices were obtained from photoelastic tests and/or from steel model tests. Dodge [2] and Rodabaugh, Dodge, and Moore [3] determined stress indices for small lug attachments, and proposed the modified term to be added in ASME Code equation to analyze such attachments. Sadd and Avent [4] developed the primary and secondary stress indices for trunnions attached to straight pipe subjected to internal pressure and moment loadings, and these stress indices B_1, C_1, B_2, C_2 were developed in terms of d/D and D/T, D/T, t/T and d/D, d/D respectively. Williams and Lewis [5] provided the primary stress indices B_1 and C_1 of trunnion elbow supports for internal pressure. Hankinson, Budlong and Albano [6] developed the secondary stress indices of trunnion elbow supports in terms of D/T, d/D and t/T for in-plane moment, out-of-plane moment and torsional moment, respectively. The purpose of this paper is to develop the primary stress indices (B_1, B_2), the secondary stress indices (C_1, C_2) and the peak stress indices (K_1, K_2) of the trunnion pipe support in terms of the dimensionless ratio (D/T, d/D, t/T, d/t) under pressure and moment loadings.

2. 3-D Finite Element Analysis

The finite element mesh was generated using the 3-D isoparametric solid element (solid 45 of ANSYS) which has eight nodal points with three degrees of freedom at each node, except one region between run pipe and trunnion supports, where solid 45 tetrahedra element was used. Because of the symmetry of the model about the longitudinal Y-Z plane (Fig. 2), a half finite element mesh was generated to reduce the wave front used in the matrix solution. The ANSYS preprocessor (PREP7) was used in generating the overall mesh. This preprocessor is an extended capability version of the node and element generation routine in the ANSYS program [7]. The mesh was generated in several segments. The three elements through the thickness were used in all regions except in the trunnion support where 2 elements through the wall were considered. In the circumferential(θ) direction, the run pipe had one element every 10 degrees and the trunnion support had one element every 5 degrees. In the longitudinal direction, the run pipe had 18 element and trunnion support consisted of 10 segments(Fig. 3).

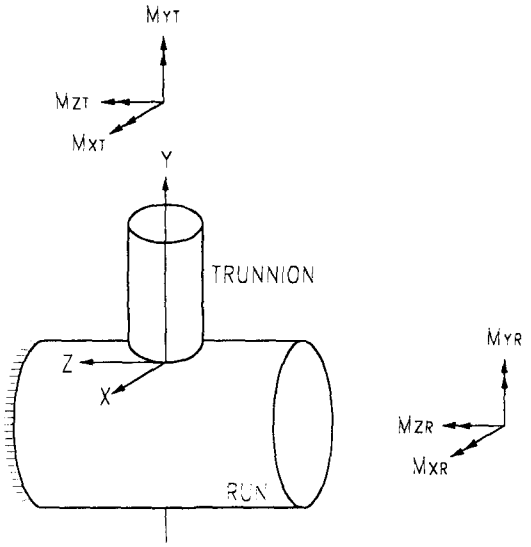

Fig. 2. Moment Loadings for Trunnion Component

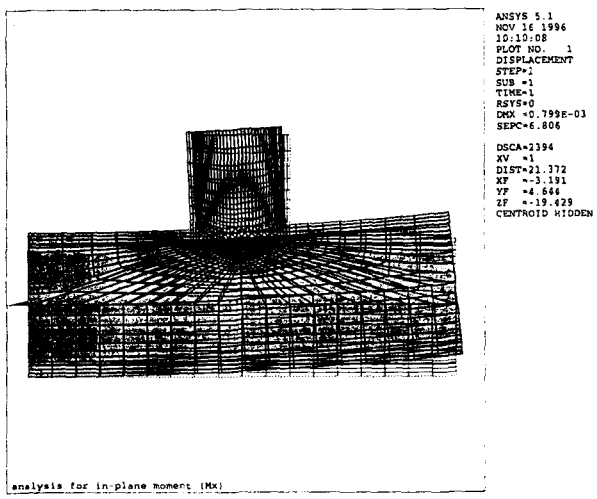

Fig. 3. Deformed and Undeformed Plot

For the elastic analysis of the trunnion pipe support, a modulus of elasticity 'E' of 206839.5 Mpa

Table 1. Dimensional Parameters

Model No.	Run Pipe					Trunnion Support					d/D	t/T
	NPS mm(inch)	Sch. N(No.)	D mm(inch)	T mm(inch)	D/T	NPS mm(inch)	Sch No.	d mm(inch)	t mm(inch)	d/t		
1	101.6(4)	40	114.30(4.500)	6.02(0.237)	19.0	76.2(3)	80	88.9(3.500)	7.62(0.300)	11.7	0.78	1.27
2	152.4(6)	40	168.30(6.625)	7.11(0.280)	23.7	101.6(4)	80	114.3(4.500)	8.56(0.337)	13.4	0.68	1.20
3	152.4(6)	80	168.30(6.625)	10.97(0.432)	15.3	101.6(4)	80	114.3(4.500)	8.56(0.337)	13.4	0.68	0.78
4	203.2(8)	40	219.08(8.625)	8.18(0.322)	26.8	101.6(4)	120	114.3(4.500)	11.13(0.438)	10.3	0.52	1.36
5	203.2(8)	80	219.08(8.625)	12.70(0.500)	17.3	101.6(4)	40	114.3(4.500)	6.02(0.237)	19.0	0.52	0.47
6	254.0(10)	40	273.05(10.750)	9.27(0.365)	29.5	152.4(6)	80	168.3(6.625)	10.97(0.432)	15.3	0.62	1.18
7	254.0(10)	60	273.05(10.750)	12.70(0.500)	21.5	152.4(6)	40	168.3(6.625)	7.11(0.280)	23.7	0.62	0.56
8	304.8(12)	40	323.85(12.750)	10.31(0.406)	31.4	254.0(10)	80	273.1(10.750)	15.09(0.594)	18.1	0.84	1.46
9	304.8(12)	60	323.85(12.750)	14.27(0.562)	22.7	203.2(8)	60	219.1(8.625)	10.31(0.406)	18.1	0.68	0.72
10	304.8(12)	120	323.85(12.750)	25.40(1.000)	12.8	203.2(8)	80	219.1(8.625)	12.70(0.500)	17.3	0.68	0.50
11	355.6(14)	30	355.60(14.000)	9.53(0.375)	37.3	152.4(6)	80	168.3(6.625)	10.97(0.432)	13.9	0.47	1.15
12	355.6(14)	30	355.60(14.000)	9.53(0.375)	37.3	203.2(8)	120	219.1(8.625)	18.26(0.719)	12.0	0.62	1.92
13	406.4(16)	60	406.40(16.000)	16.66(0.656)	24.4	203.2(8)	40	219.1(8.625)	8.18(0.322)	26.8	0.54	0.49
14	508.0(20)	40	508.00(20.000)	15.09(0.594)	33.7	254.0(10)	80	273.1(10.750)	15.09(0.594)	18.1	0.54	1.00
15	508.0(20)	40	508.00(20.000)	15.09(0.594)	33.7	406.4(16)	30	406.4(16.000)	9.53(0.375)	42.7	0.80	0.63

NPS : Nominal Pipe Size

Sch. No. : AMSI B36.10 steel pipe schedule numbers

(30×10^6psi) and a Poission's ratio 'ν' of 0.3 were used for both cases of the loadings : internal pressure and moment.

A pressure of 6.895 MPa(1000 psi) was applied on all exposed internal surfaces of the run pipe. The moment of 1130 N-m(10000 lb-in) was given on run pipe and trunnion support. The boundary membrane forces were applied as a negative(tensile) pressure at the right end of the run pipe. For the bending moment loadings, linear varying loads producing the proper statically equivalent effect were applied at the ends of the run pipe and trunnion support. Twisting moments were generated by a uniform distribution of tangential loading at the ends. A half symmetric model was utilized for all analyses. This modeling technique exploited each structure's geometrical symmetry with respect to the plane of the pipe's longitudinal axis. Compatibility of the nodal deformation between the half model and the equivalent whole model was maintained by specifying symmetric displacement fields.

3. Stress Analysis Results

The run pipe and trunnion support dimensions for the representative models under consideration are given in Table 1. From the dimensional parameters outlined in Table 1, stress indices are later developed in terms of selected non-dimensionl parameters.

For all models, displacements (Ux, Uy and Uz) were calculated at all nodal points. In addition, stress components (σ_x, σ_y, σ_z, σ_{xy}, σ_{yz} and σ_{xz}), principal stresses, and the maximum shear stresses were calculated at all nodal points. Displacements and stress contour plots were obtained for the Model No. 10 using the 3 dimensional solid element post-processor (POST 1) of ANSYS. These plots are intended to provide an understanding of the pattern of stress distribution in the model. Displacement plot under moment loading is presented in Figure 3. In all of the displacement plots, the dashed lines show the undeformed or original configulation and the solid lines indicate the deformed shapes. The stress intensity (σ) is defined to be twice the maximum shear stress or simply the difference between the algebraically largest and smallest principal stresses. The stress intensity contour about moment is shown on Figure 4. The maximum and minimum stress values based on extrapolated values are indicated on the plots by 'MN' and 'MX', respectively.

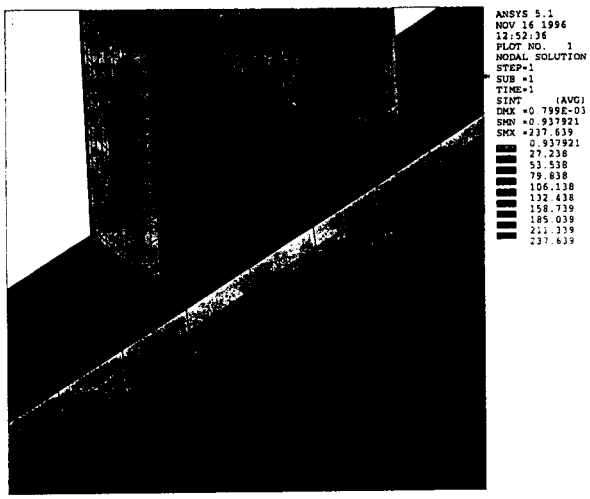

Fig. 4. Stress Intensity Plot

4. Stress-Index Development

To provide designers with a rapid approximate analysis, the ASME Code Sec. Ⅲ, recommends a stress-index and stress-intensity method. These methods categorize the total stress at any point in the structure into primary, secondary and peak stress components. Loadings are also classified into pressure, moment and thermal types. These simplified design stress formulas involve terms containing a stress index multiplied by a nominal stress. Hence these formulas allow a designer to rapidly check for allowable stresses with previously computed stress indices.

The definitions of primary stress, secondary stress and peak stress are included in reference [1] : Primary stress is any stress developed by an imposed loading which is necessary to satisfy the laws of equi-

librium. The basic characteristic of a primary stress is that it is not self-limiting. Secondary stress is a stress developed by the constraint of adjacent material or by self-constraint of the structure. The basic characteristic of a secondary stress is that it is self-limiting. Peak stress is that increment of stress which is additive to the primary plus secondary stresses by reason of local discontinuities including the effects, if any, of stress concentrations. The basic characteristic of a peak stress is that it does not cause any noticeable distortion and is objectionable only as a possible source of a fatigue crack or a brittle fracture.

ASME Code Section Ⅲ of the ASME Boiler and Pressure Vessel Code provides the definition of a stress index to be

$$B, C \text{ or } K = \sigma/S \quad (1)$$

where B = Primary stress index
C = Secondary stress index
K = Peak stress index
σ = Elastic stress intensity due to a load
S = Nominal stress due to a load

The three types of stress indices represented by B, C and K are defined by the Code to be primary, secondary and peak indices, respectively. Each of the three categories of stress indices are further subdivided according to the manner of loading and are identified by the subscripts 1, 2 and 3, which signify pressure, bending and thermal loads, respectively.

For B index, σ represents the stress magnitude corresponding to the limit load. For C or K indices, σ represents the maximum stress intensity due to applied load. The nominal stress for isothermal conditions are

$$S = PD/(2T) \text{ ; pressure loading} \quad (2)$$

$$S = MiD/(2I) \text{ ; moment loading} \quad (3)$$

where P = Internal pressure
D = Outside diameter of run pipe
T = Thickness of run pipe
M_i = Applied moment
I = Area moment of inertia of pipe cross section

The stress values computed by finite element analysis simply give a total stress which is composed of the primary, secondary and peak components. For the current study, the ANSYS Solid 45 element allow to categorize of the total stress into membrane and bending components (LPATH command in ANSYS classifies membrane, bending and peak stress.). Consequently, the membrane values were used to determine B_1 and B_2, the membrane plus bending portion were used to determine C_1 and C_2 , and the total stress were used to determine K_1 and K_2.

As mentioned before, it is desired to compute the largest stress index for each component studied, and then to develop an empirical equation expressing this controlling index in terms of particular non-dimensionl parameters. Table 2 shows the maximum stress indices for the various loadings. Results are given for both the trunnion and run pipes. Locations of these maximum values generally occured near the intersection zone.

The following relationship was used to derive stress indices for pressure and moment loadings :

$$B_1, C_1 \text{ or } K_1 = A_0 (D/T)^{m1} (d/D)^{m2} (t/T)^{m3}$$
$$B_2, C_2 \text{ or } K_2 = A_0 (d/t)^{m1} (D/T)_m^2 (d/D)^{m3} (t/T)^{m4} \quad (4)$$

where D = Outside diameter of run pipe
d = Outside diameter of trunnion pipe support
T = Thickness of run pipe
t = Thickness of trunnion pipe support
A_0 = Constant
m_1, m_2, m_3, m_4 = Exponent

In order to determine the B_1, B_2, C_1, C_2, K_1 and K_2 indices in terms of the dimensional parameters given in Table 1, the maximum primary, maximum primary plus secondary and maximum total stress intensities were chosen for each model. The following equations (5) to (16) for B_1, B_2, C_1, C_2, K_1 and K_2 indices

Table 2. Dimensional Parameters

Model				Run Pipe									Trunnion Support								
No.	B_1	C_1	K_1	B_{2x}	B_{2y}	B_{2z}	C_{2x}	C_{2y}	C_{2z}	K_{2x}	K_{2y}	K_{2z}	B_{2x}	B_{2y}	B_{2z}	C_{2x}	C_{2y}	C_{2z}	K_{2x}	K_{2y}	K_{2z}
1	0.981	1.210	1.016	0.965	1.054	0.850	1.272	1.122	1.151	1.033	0.996	1.044	4.174	2.433	4.070	6.619	3.435	13.83	1.027	0.953	1.241
2	0.975	1.229	0.991	0.967	1.067	0.897	1.200	1.118	1.183	1.027	0.997	1.023	4.685	2.413	4.301	7.389	3.364	17.74	1.039	1.041	1.144
3	0.958	1.145	1.014	0.949	1.039	0.866	1.197	1.125	1.177	1.034	0.995	1.047	2.353	2.454	2.283	3.938	3.174	7.716	1.044	1.045	1.208
4	0.962	1.250	1.033	0.986	1.074	0.962	1.201	1.116	1.182	1.024	0.998	1.019	4.489	2.203	4.214	8.148	3.120	19.94	1.016	1.057	1.087
5	0.953	1.149	1.018	0.942	1.047	0.938	1.090	1.130	1.145	1.028	0.995	1.034	2.038	2.377	1.332	3.639	2.893	5.293	1.027	1.028	1.116
6	0.972	1.270	0.994	0.969	1.089	0.939	1.149	1.117	1.175	1.023	0.997	1.019	4.814	2.415	4.663	8.428	3.343	21.60	1.014	1.033	1.105
7	0.971	1.135	1.021	0.946	1.062	0.931	1.078	1.119	1.152	1.028	0.997	1.031	2.344	2.542	2.016	3.765	3.206	8.088	1.027	1.019	1.134
8	1.010	1.278	1.001	0.955	1.086	0.861	1.170	1.122	1.138	1.024	0.998	1.036	7.194	2.546	6.713	10.87	3.796	25.53	1.021	1.023	1.205
9	0.979	1.143	1.015	0.951	1.065	0.909	1.106	1.118	1.166	1.029	0.997	1.031	2.753	2.608	2.789	4.683	3.393	10.98	1.059	1.021	1.157
10	0.953	1.137	1.019	0.926	1.022	0.872	1.128	1.127	1.153	1.032	0.994	1.059	1.989	2.424	1.398	3.421	2.971	4.360	1.026	1.034	1.233
11	0.972	1.285	1.006	0.981	1.094	0.991	1.116	1.124	1.158	1.018	0.998	1.015	4.715	2.296	4.379	8.801	3.092	23.23	1.013	1.034	1.066
12	0.974	1.286	1.017	0.995	1.096	0.971	1.186	1.124	1.184	1.010	0.998	1.007	8.302	3.965	8.046	14.34	4.309	41.27	1.017	1.005	1.081
13	0.971	1.155	1.001	0.952	1.070	0.956	1.058	1.118	1.129	1.026	0.997	1.025	2.265	2.453	1.741	3.726	3.045	7.732	1.024	1.017	1.099
14	0.980	1.280	0.996	0.971	1.092	0.968	1.108	1.121	1.159	1.020	0.998	1.017	4.227	2.452	4.037	7.726	3.278	20.11	1.013	1.024	1.081
15	1.008	1.192	1.046	0.951	1.095	0.914	1.037	1.120	1.124	1.024	0.998	1.023	2.487	2.723	3.505	4.770	3.745	13.92	1.154	1.005	1.175

were derived from the results of numerical data in Table 2. All results presented here are proposed only for the dimensional ranges $10 \le D/T \le 40$, $0.47 \le d/D \le 0.84$, $0.5 \le t/T \le 2.0$. Fig. 5 to 10 show the comparison between finite element analysis and Eqns. (5) to (16) curve-fitted.

$$B_{1M} = 0.953\,(D/T)^{0.0169}\,(d/D)^{0.0543}\,(t/T)^{0.00915} \text{ for } (t/T) \ge 1 \quad (5)$$

$$B_{1M} = 0.953\,(D/T)^{0.0169}\,(d/D)^{0.0543}\,(t/T)^{0.0319} \text{ for } (t/T) < 1 \quad (6)$$

$$C_{1M} = 0.829\,(D/T)^{0.111}\,(d/D)^{-0.0445}\,(t/T)^{0.0185} \text{ for } (t/T) \ge 1 \quad (7)$$

$$C_{1M} = 0.829\,(D/T)^{0.111}\,(d/D)^{-0.0445}\,(t/T)^{0.00829} \text{ for } (t/T) < 1 \quad (8)$$

$$K_{1M} = 1.085\,(D/T)^{-0.0208}\,(d/D)^{0.00736}\,(t/T)^{0.0358} \text{ for } (t/T) \ge 1 \quad (9)$$

$$K_{1M} = 1.085\,(D/T)^{-0.0208}\,(d/D)^{0.00736}\,(t/T)^{0.0126} \text{ for } (t/T) < 1 \quad (10)$$

$$B_{2M} = 0.946\,(d/t)^{-0.0339}\,(D/T)^{0.457}\,(d/D)^{0.173}\,(t/T)^{1.202} \text{ for } (t/T) \ge 1 \quad (11)$$

$$B_{2M} = 0.946\,(d/t)^{-0.0339}\,(D/T)^{0.457}\,(d/D)^{0.173}\,(t/T)^{0.253} \text{ for } (t/T) < 1 \quad (12)$$

$$C_{2M} = 0.585\,(d/t)^{0.266}\,(D/T)^{0.720}\,(d/D)^{-0.254}\,(t/T)^{1.460} \text{ for } (t/T) \ge 1 \quad (13)$$

$$C_{2M} = 0.585\,(d/t)^{0.266}\,(D/T)^{0.720}\,(d/D)^{-0.254}\,(t/T)^{0.939} \text{ for } (t/T) < 1 \quad (14)$$

$$K_{2M} = 1.690\,(d/t)^{0.0534}\,(D/T)^{-0.132}\,(d/D)^{0.223}\,(t/T)^{0.0222} \text{ for } (t/T) \ge 1 \quad (15)$$

$$K_{2M} = 1.690\,(d/t)^{0.0534}\,(D/T)^{-0.132}\,(d/D)^{0.223}\,(t/T)^{0.0855} \text{ for } (t/T) < 1 \quad (16)$$

where B_{1M} = Modified primary stress index due to internal pressure

B_{2M} = Modified primary stress index due to moment

C_{1M} = Modified secondary stress index due to internal pressure

C_{2M} = Modified secondary stress index due to moment

K_{1M} = Modified peak stress index due to internal pressure

K_{2M} = Modified peak stress index due to moment

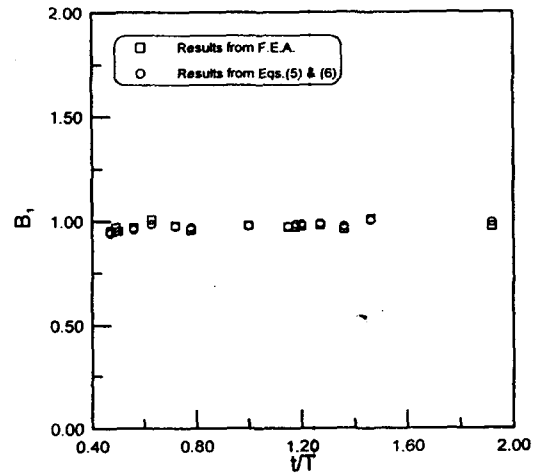

Fig. 5. Comparison of the Results From F.E.A. vs Eqs. (5) & (6) for B_1

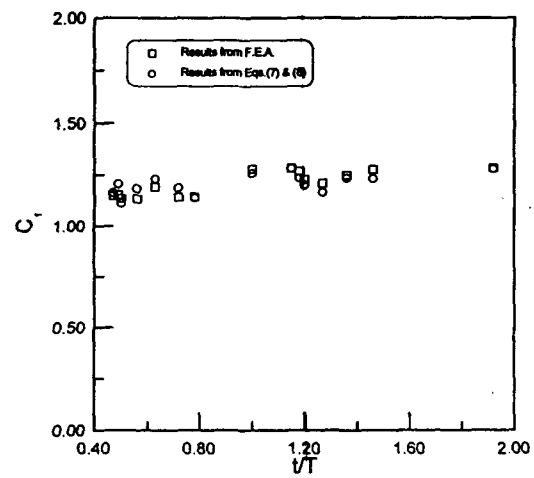

Fig. 6. Comparison of the Results from F.E.A. vs Equ. (7) & (8) for C_1

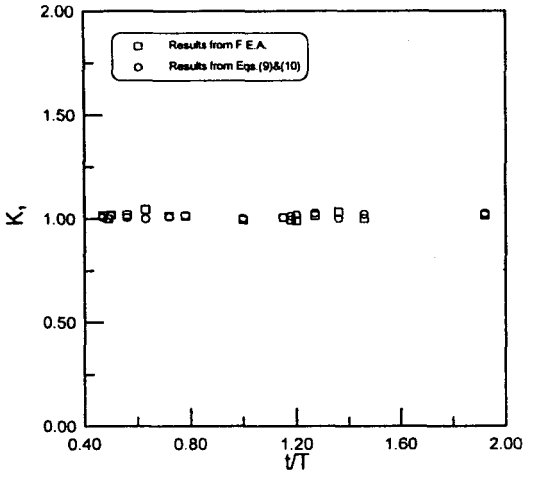

Fig. 7. Comparison of the Results from F.E.A. vs Eqs. (9) & (10) for K_1

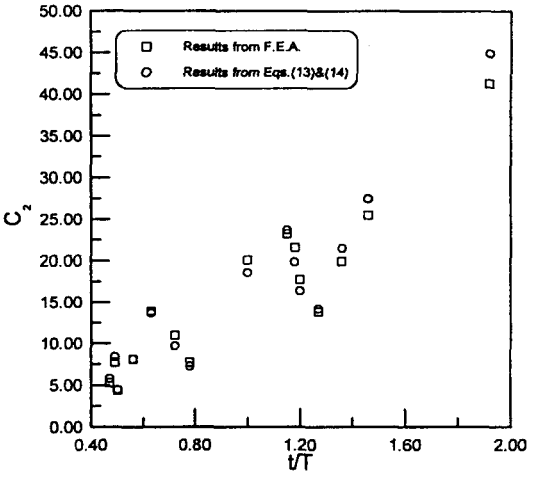

Fig. 9. Comparison of the Results from F.E.A. vs Eqs. (13) & (14) for C_2

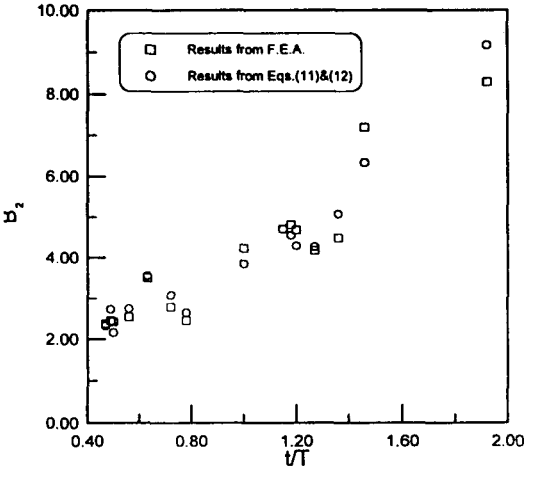

Fig. 8. Comparison of the Results from F.E.A. vs Equ. (11) & (12) for B_2

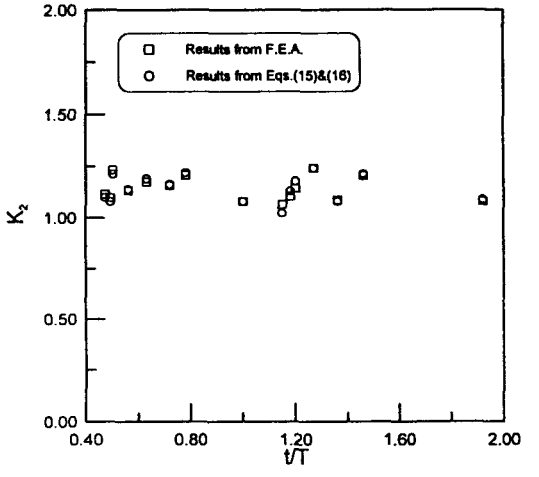

Fig. 10. Comparison of the Results from F.E.A. vs Eqs. (15) & (16) for K_2

5. Discussions

When the attachments such as lugs or trunnion supports are attached to the piping, the ASME Code Case [8] is recommened to evaluate the integrity of the piping system. Eq. (17) shows the primary plus secondary stress intensity except the thermal term in ASME Sec.III NB-3653.1. The stress indices derived in this paper are used in Eq. (17). Eq. (18) used in the ASME Code Case N-391-1 represents the evaluation equation for attachments on piping.

$$C_{1M}(PD/2T) + C_{2M}(M_iD/2I) \quad (17)$$

$$C_1(PD/2T) + C_2(M_iD/2I) + S_{NT} \quad (18)$$

where S_{NT} = Local stress (primary and secondary stress) for attachments

Table 3. Comparison between Eq. (17) and Eq. (18)

	Eq. (17)	Eq. (18)
Model 7 pipe : 10″ sch.60 sup't : 6″ sch.40	12.90 psi	11.82 psi
Model 10 pipe : 12″ sch.120 sup't : 8″ sch.80	7.18 psi	6.65 psi
pipe : 8″ sch.80 sup't : 6″ sch.40	10.34 psi	9.70 psi
pipe : 12″ sch.60 sup't : 6″ sch.40	13.42 psi	12.32 psi

Table 4. Comparison between Eq. (19) and Eq. (20)

	Eq. (19)	Eq. (20)
Model 7 pipe : 10″ sch.60 sup't : 6″ sch.40	13.23 psi	12.65 psi
Model 10 pipe : 12″ sch.120 sup't : 8″ sch.80	7.32 psi	6.85 psi
pipe : 8″ sch.80 sup't : 6″ sch.40	10.57 psi	10.42 psi
pipe : 12″ sch.60 sup't : 6″ sch.40	13.88 psi	13.08 psi

To evaluate the equations (17) and (18), the pressure of 6.895 kPa(1 psi) and moments of 0.113 N-m(1 lbs-in) are applied. Two examples (model 7 & 10) shown on Table 3 & 4 are selected from Table 1 and remaining two examples shown on Table 3 & 4 are selected from arbitrary piping with trunnion attachment to compare the stress results of the proposed equations with those of the ASME Code Case N-391-1.

Table 3 shows that the stress results of Eq. (17) derived in this paper have good agreement with those of the ASME Code Case N-391-1 for secondary stress. The maximum deviation in Table 3 is within 10%.

Eq. (19) shows the peak stress intensity except the thermal term in ASME Sec.III NB-3653.2. The stress indices derived in this paper are used in Eq. (19). Eq. (20) used in the ASME Code Case N-391-1 represents the evaluation equation for attachments on piping.

$$K_{1M}C_{1M}(PD/2T) + K_{2M}C_{2M}(M_iD/2I) \quad (19)$$

$$K_1C_1(PD/2T) + K_2C_2(M_iD/2I) + S_{PT} \quad (20)$$

where S_{PT} = Local stress(primary, secondary and peak stress) for attachments

Table 4 shows that the stress results of Eq. (19) derived in this paper also have good agreement with those of the ASME Code Case N-391-1 for peak stress. The maximum deviation in Table 4 is within 10%.

The current procedure of evaluating the local stress for attachments is followed ;

First, the piping system stress is determined by ASME Code NB-3653 for straight pipe (without attachments). Second, the result of straight pipe is used to perform the local stress for attachments. The complicate equation for the local stress is given in ASME Code Case N-391-1. Therefore, the evaluation of local stress is determined by two steps.

Because the pipe and attachment are analyzed with together, the empirical equations derived in this paper contain the result of the local stress. If the dimensional parameters of the pipe and attachment are given, the integrity of piping systems with attachments is evaluated directly. Therefore, the use of empirical equations (5) to (16) can simplify the procedure of evaluating the local stress.

6. Conclusions

Stress analysis and stress index results have been presented for a trunnion pipe supports when loaded by internal pressure and moments. The component was analyzed as a three-ended branch component, and the stresses were categorized by loading type and Code decomposition (Primary, Secondary and

Peak).

The empirical equations were developed for the B_1, B_2, C_1, C_2, K_1 and K_2 indices. The maximum deviation between the empirical equations and Code Case results is within 10 percent. All results presented here are proposed only for the dimensional ranges $10 \leq D/T \leq 40$, $0.47 \leq d/D \leq 0.84$, $0.5 \leq t/T \leq 2.0$.

Based on the comparison between stress value by stress indices derived in this paper and stress value represented by the ASME Code Case N-391-1, the empirical equations for stress indices are effectively used in the piping stress analysis.

The current procedure of evaluating the local stress for attachments is determined by two steps. But, the empirical equations (5) to (16) evaluate the local stress directly. Therefore, the use of empirical equations can simplify the procedure of evaluating the local stress in the piping design stage.

References

1. ASME Boiler and Pressure Vessel Code, Section Ⅲ. Division 1, "Nuclear Power Plant Components", American Society of Mechanical Engineers, New York, Edition (1989)
2. W.G. Dodge, "Secondary Stress Indices for Integral Attachments to Straight Pipe", Welding Research Council Bulletion 198, Sept. (1974)
3. E.C. Rodabaugh, W.G. Dodge, and S.E. Moore, "Stress Indices at Lug Supports on Piping Systems", Welding Research Council Bulletion 198, Sept. (1974)
4. M.H. Sadd and R.R. Avent, "Stress analysis and stress index development for a trunnion pipe support", ASME Journal of Pressure Vessel Technology, Vol. 104, No. 2, pp. 73-78. May (1982)
5. D.K. Williams and G.D. Lewis, "Development of B_1 and C_1 stress indices for trunnion elbow supports", ASME Journal of Pressure Vessel Technology, Vol. 106, No. 2, pp. 166-171 May (1984)
6. R.F. Hankinson, L.A. Budlong and L.D. Albano, "Stress indices for piping elbows with trunnion attachments for moment and axial loads", ASME PVP-Vol. 129, pp 43-49 (1987)
7. ANSYS Engineering Analysis System User's Manual for Revision 5.1, Swanson Analysis System, Houston, Pa., (1994)
8. ASME Code Case N-391-1 "Procedure for Evaluation of the Design of Hollow Circular Cross Section Welded Attachments on Class 1 Piping", July (1989)
9. C.F. Gerald and P.O. Wheatley, Applied Numerical Analysis, pp 530-576, 3th ed., Addison Wesey, (1984)